Forward-Scattering Enhancement of Comet Brightness. III. Prospects for C/2010 (Elenin) as Viewed from the Earth and the SOHO, STEREO-A, and STEREO-B Spacecraft

Joseph N. Marcus
19 Arbor Road
St. Louis, MO 63132 USA
josephnmarcus@gmail.com

Submitted to International Comet Quarterly *2011 July 28*

Abstract

Comet C/2010 X1 (Elenin) ventures into extreme forward-scattering geometry when it passes between the Sun and the STEREO-B spacecraft (minimum scattering angle $\theta_{min} = 7.3°$ on Aug. 13.13 UT), the Earth ($\theta_{min} = 3.1°$ on Sept. 26.78 UT), and the SOHO spacecraft ($\theta_{min} = 3.1°$ on Sept. 26.90 UT). Near these times, brightness enhancements of –6 to –7 magnitudes from the baseline can be expected, based on a model of the coma scattering function, $\Phi(\theta)$ (Marcus 2007a). Large as they are, these predicted enhancements are blunted by the comet's extremely low dust-to-gas light ratio, inferred as $\delta_{90} = 0.15$ from current continuum photometry. I analyze current visual magnitudes through June and develop a model for a baseline light curve which incorporates a dust-to-gas light ratio, $\delta_{90}(r)$, which varies with heliocentric distance, r. The model predicts a falloff in the index of brightening of C/2010 X1 from n = 4 at r > 1 AU to n = 3 at r < 1 AU in the canonical baseline total magnitude formula $m_1 = H_0 + 5 \log \Delta + 2.5\ n \log r + m_{\Phi(\theta)}$, where $m_{\Phi(\theta)} = -2.5 \log \Phi(\theta)$, Δ is comet-observer distance, and $H_0 = 8.0$ is the derived absolute magnitude. I provide ephemerides with predicted forward-scattering magnitude enhancement, $m_{\Phi(\theta)}$, and total magnitude, m_1, for C/2010 X1 as viewed from Earth, SOHO, STEREO-A and STEREO-B. At small θ, the coma and tail are likely to be prominent and even spectacular as viewed from the STEREO-B and SOHO. However, owing to the comet's faint H_0 and small elongations and interfering twilight, the forward-scattering enhancement is not likely to be detected from Earth, nor is the comet likely to be detected in daylight at θ_{min}, based on a model developed in a companion paper (Marcus 2011). The simultaneous observations of C/2010 X1 from different locations in space offers an unprecedented opportunity to define the coma scattering function at small scattering angles.

1. Introduction

Forward-scattering of sunlight by dust in a comet's coma and tail produces dramatic brightening, a phenomenon which has not been widely recognized in the comet science community until recently. In Paper I of this series (Marcus 2007a), I presented a model for forward-scattering brightness enhancement in comets, and applied it to successfully predict

(Marcus 2007b) – and in Paper II, analyze (Marcus 2007c) – the brightness surge and daylight visibility of comet C/2006 P1 (McNaught). Subsequently this model was applied by Knight et al. (2010) to analyze and correct the brightness statistics of the small Kreutz comets detected by the C2 and C3 coronagraphs aboard Solar Heliospheric Observatory (SOHO) satellite between 1996-2005.

Leonid Elenin, Lyubertsy, Moscow region, Russia, discovered Comet C/2010 X1 on images taken remotely on 2010 Dec. 10.44 UT with the 0.45-m f/2.8 astrograph at the ISON-NM Observatory at Mayhill, New Mexico (MPC *Circular* 73016, 2011 Jan. 19). It was then Δ = 4.304 from Earth and r = 4.216 from the sun. The comet reaches perihelion on T = 2011 Sept. 10.72 TT at q = 0.482 AU (Williams 2011). Because its orbit is nearly coincident with the ecliptic plane (i = 1.84°), the comet enters deep forward-scattering geometry not only as viewed from the Earth, but also from two sun-monitoring spacecraft, SOHO and the STEREO-B. This circumstance presents an unprecedented opportunity to observe the comet simultaneously from at least two different positions, and thereby derive the comet dust scattering function to high precision at small scattering angles.

In this, Paper III of the series, I will first derive the "baseline" brightness of C/2010 X1. This is a particular challenge because of the extremely low dust-to-gas ratio which has been reported for this comet (Section 2.2), and so in Section 2.1 I devise a novel model to predict the effect of this ratio, which varies with heliocentric distance, on the comet's baseline light curve, which is presented and analyzed in Sections 2.3-2.6. The forward-scattering model is reviewed in Section 3, and pertinent details of the SOHO and STEREO spacecraft are presented in Section 4. In Section 5 I provide ephemerides for the comet as based from Earth, STEREO-B, and SOHO, as well as for STEREO-A, which is currently in solar orbit at earth's distance opposite the Sun from STEREO-B. The ephemerides provide the comet's location, the expected degree of forward-scattering brightness enhancement as a function of the scattering angle, θ (= 180° – β, where β is the phase angle), and the total magnitude. Finally, in Section 6 I apply a model for the daylight visibility of comets, presented as a companion paper (Marcus 2011), to assess whether Comet Elenin can become visible in daylight from the Earth in extreme forward-scattering geometry.

2. The Baseline Brightness of C/2010 X1

2.1 Model

The total brightness of a comet, which I denote below with a subscript "1," is a combination of contributions sunlight scattered from the dust and fluorescence emission from the gas (predominantly C_2):

$$I_1(r) = I_{dust}(r) + I_{gas}(r) = I_{dust}(r)\left[1 + \frac{1}{\delta_{90}(r)}\right], \qquad (1)$$

where $\delta_{90}(r) = I_{dust}(r)/ I_{gas}(r)$ is the dust-to-gas light ratio, as viewed at θ = 90°, at a given heliocentric distance, r. In a literature review in Section 3.5 of Paper I (Marcus 2007a), I found that the relation

$$\delta_{90}(r) = \delta_{90}\,\frac{r^{-1} + r^{-2}}{2} \tag{2}$$

fits an ensemble of observations rather well. Here δ_{90}, the dust-to-gas light ratio at r = 1 AU, is 1 for an "average" comet, while $\delta_{90} > 1$ for "dusty" and $\delta_{90} < 1$ for "gassy" comets. Dust production in comets commonly scales to $r^{-\alpha}$ over a wide range of r. By the inverse square law, the brightness of any optically apparent dust present in the coma scales to r^{-2}, so that

$$I_{dust}(r) = (I_{dust})_0\, r^{-\alpha-2} = (I_{dust})_0\, r^{-m} = I_0\left[1 + \frac{1}{\delta_{90}}\right]^{-1} r^{-m}, \tag{3}$$

where $(I_{dust})_0$ and I_0 are respectively the dust and the total brightnesses at r = 1 AU and $m = \alpha + 2$ is the index of dust brightening. Substituting for $I_{dust}(r)$ and $\delta_{90}(r)$, Equation 1 becomes

$$I_1(r) = I_0 r^{-m}\left[1 + \frac{1}{\delta_{90}(r)}\right]\left[1 + \frac{1}{\delta_{90}}\right]^{-1}. \tag{4}$$

The corresponding heliocentric total magnitude is

$$H_1(r) = -2.5\log H_1(r) = H_0 + 2.5m\log r - 2.5\log\left[\frac{1 + \delta_{90}(r)^{-1}}{1 + \delta_{90}{}^{-1}}\right], \tag{5}$$

where $H_0 = -2.5 \log I_0$ is the absolute total heliocentric magnitude defined at r = 1 AU.

Because α typically is close to 2, Equation 3 leads to the inverse fourth power relation $I_{dust}(r) \propto r^{-4}$. To the extent that $\delta_{90}(r)$ remains constant in Equation 2, the dependence of $I_1(r)$ on r will *parallel* that of $I_{dust}(r)$, that is, $I_{dust}(r) \propto I_1(r) \propto r^{-n}$, where n is the index of brightening of $I_1(r)$ and $n \approx m \approx 4$, producing the familiar canonical inverse fourth power law for *total* comet brightness as well. The condition that $n \approx m$ holds well for $0.5 \text{ AU} \le r \le 1.2$ AU, where $\delta_{90}(r)$ in Equation 2 remains fairly constant. Outside of this interval, however, $n < m$ for $r < 0.5$ AU and $n > m$ for $r > 1.2$ AU. The inequality between n and m is accentuated for gassy comets ($\delta_{90} < 1$) but may be barely noticed for dusty comets ($\delta_{90} > 1$).

This method of modeling the total brightness and magnitude of a comet in terms of its dust component is novel and its principles perhaps less unfamiliar to analysts. However, for the purpose of forecasting the baseline total brightness of C/2010 X1, it assumes importance because of data discussed in the next section.

2.2 Continuum Photometry and the Dust-to-Gas Light Ratio (δ_{90})

The CARA group reports very small values for the Afρ parameter, a measure of dust content in the coma, for C/2010 X1 (Sostero and Milani 2011). Derived from broadband CCD continuum photometry, their data show steady or even slightly decreasing Afρ values with decreasing heliocentric distance from March through mid-May, although their data were not adjusted for backscattering occurring in the weeks around opposition, which occurred on Mar. 14. David G. Schleicher, Lowell Observatory, obtained photoelectric photometry of C/2010 X1 on June 28 UT, and found no measurable counts in the narrowband continuum filters. In a very preliminary analysis, he places rough 1-sigma upper limits on log Afρ as 1.4, and on its ratio with the OH production rate, Q, as log Afρ/log Q[OH] = –26.3, which he characterizes as "very gassy" (M. Knight and D. Schleicher, Lowell Observatory, personal communication). He remarks that this value is essentially the same as the –26.4 ratio found for the extremely gassy comet 2P/Encke (A'Hearn et al. 1995). Newburn (1981) found that the dust-to-gas light ratio at 90°, reflecting the strengths of continuum to C_2 emissions in the scotopic visual bandpass, was $\delta_{90} = 0.13$ for 2P/Encke, among the lowest of any comet. For a "typical" comet, $\delta_{90} = 1$, and for a very dusty one, $\delta_{90} >> 1$ (Marcus 2007a). For C/2010 X1, I adopt $\delta_{90} = 0.15$, close to that for 2P/Encke, in the analysis which follows.

2.3 CCD and Visual Total Magnitudes (m_1)

To construct a light curve, I utilize unfiltered CCD magnitudes (over 2.8 AU ≤ r ≤ 4.2 AU) and visual (m_1) magnitudes (over 1.6 AU ≤ r ≤ 2.9 AU) reported to the International Comet Quarterly and kindly supplied in unchecked form by D. W. E. Green. The CCD observers and/or measurers (with ICQ code) are Artyom Novichonok (NOV01), Petrozavodsk, Russia; Katsumi Yoshimoto, Hirao, Japan (YOS02); Sergey E. Shurpakov, Baran, Belarus (SHU); Walter Kutschera, Feldatal, Germany (KUT); and Emil Březina, Czech Republic (BRE03). The visual m_1 observers are Kutschera; Jakub Koukal, Kromeriz, Czech Republic (KOU); J. J. Gonzalez, various high elevation sites, northern Spain (GON05); Jakub Černý, Senohraby, Czech Republic (CER01); Carlos Labordena, Spain; Alan Hale, New Mexico; M. Goiato, Brazil; and Alexandre Amorim, Brazil. I supplement these with more recent observations obtained from the websites CometObs (http://tech.groups.yahoo.com/group/CometObs/) and Comets-m1 (http://tech.groups.yahoo.com/group/comets-ml/), which include those of Chris Wyatt, Walcha, NSW, Australia. The m_1 estimates are derived from comparisons with the extrafocal images of stars of known magnitude. The first visual sighting, at $m_1 = 14.6$ and coma = 0.8′, was by Kutschera on Mar. 28.95 UT in a 92-cm reflector at 125×, followed by Kouchal on Apr. 1.86 UT at $m_1 = 15.3$, coma = 0.5′, in a 24-cm reflector at 133×. Up to early June the visual observations have required relatively large-aperture telescopes (≥ 20 cm) at high magnifications (100× to 240×), but in the latter half of the month they have ranged down to 39× (Wyatt). To early June the coma was up to 1.2′ diameter with the degree of condensation ranging from 3 to 7, but in the latter part of the month it has been reported as 2.5′ diameter and DC = 3 (Wyatt, Gonzalez).

2.4 Color Correction of the CCD Magnitudes

I analyze the light curve in reference to the human visual scotopic passband, considered equivalent to V. The unfiltered CCD magnitudes follow the spectral responses of the chips, which are red-sensitive. G. Sostero points out that these are essentially equivalent to the R band, and following his algorithm, I transform them to the visual passband equivalent by V = R + 0.4 (see Marcus 2007c).

2.5 Backscattering Correction of CCD and Visual m_1 Magnitudes

Because C/2010 X1 passed opposition on 2011 Mar. 14.59 UT at r = 3.099 AU and a minimum phase angle $\beta_{min} = 0.4°$, brightness enhancement from backscattering by the dust should have occurred. Accordingly, both the CCD and the visual m_1 observations, which ranged over $0.5° \leq \beta \leq 34.1°$, were corrected to a $\beta = 90° = \theta$ viewing angle using the formula $m_1(90°) = m_1 - \gamma(\beta - 20°)$. For a usual comet, $\gamma = 0.031$ magnitude deg^{-1} as derived and illustrated in Section 4.4 and Fig. 16 of Paper I (Marcus 2007a). However, given the extreme gassiness of C/2010 X1 (Section 2.2), I adopt $\delta_{90} = 0.15$ in Equation 2, and derive and apply $\gamma = 0.013$ magnitude deg^{-1} for the visual m_1 observations, and $\gamma = 0.027$ magnitude deg^{-1} for the unfiltered CCD magnitudes.

2.6 Analysis and Baseline Brightness Forecast

The total magnitude estimates, corrected for color and backscattering, are next reduced to heliocentric magnitude

$$H_1(r) = H_1 = m_1 - 5\log\Delta, \qquad (6)$$

the magnitude as viewed at earth distance $\Delta = 1$ AU, which is then plotted in Figure 1 against the logarithm of the heliocentric distance. The following analytic points and inferences can be made:

1. The aggregate slope for the CCD magnitudes is near n = 3 to 3.5. I also analyzed the CCD total magnitudes published on the Minor Planet Electronic Circulars (MPECs), a larger data set (not shown here), but taken with less photometric rigor. These latter data yield a slope of n = 3. The CCD observations should reflect dust brightness, because the observations are unfiltered and the chips have broad spectral sensitivity deep into red and near-infrared, although admittedly there may be some contamination from C_2 emission from a comet as gassy as C/2010 X1. It is reasonable to conclude that the dust brightness slope in Equations 3-5 is close to m = 3, and that the dust production rate of C/2010 X1 is anemic, with $\alpha = 1$ in Equation 3.
2. The visual m_1 estimates in Figure 1 are systematically brighter than the CCD magnitudes by about 1 to 1.5 magnitudes at log r = 0.45. This is not a surprise, as this disparity is frequently seen in the photometry of faint comets. It may owe to the failure of the CCD photometry to fully integrate the faint outer extent of the comas of faint comets, as suggested by Ferrín (2005), and to the greater relative contribution of

any C_2 Swan bands to the human scotopic visual passband in comparison to the broader unfiltered CCD passbands.

3. The three observers with the four or more visual m_1 estimates (Koukal, Černý and Gonzalez) are remarkably interconsistent, with a scatter range of only about 0.5 magnitude. C/2010 X1 has been a very faint, diffuse and difficult object that has eluded many experienced observers, so the interconsistency among these three prolific and experienced observers is reassuring.
4. The visual m_1 observations show a sharp upslope of n = 4 to 5, greater than that of the m = 3 dust slope. That n > m in this range of r is a predicted consequence of increasing relative C_2 emission in the model as discussed in Section 2.1.

Any magnitude forecast derived from these data should reflect the comet as it would be seen in the coming months in the large-scale STEREO and SOHO spacecraft camera fields and by observers on Earth using low-power binoculars and (hopefully) the naked eye. The problem is, the current observations are at high magnifications in intermediate-aperture telescopes. As such, they likely are affected by "magnification artifact" (or "aperture effect": Morris 1973), wherein under the high magnification attending larger apertures, the contrast gradient of the faint outer coma falls below the threshold of the visual nervous system, forcing the perceived outer boundary of the physical coma to move *inward*, and causing a dimmer m_1 estimate. This paradoxical contraction of the coma with larger apertures and magnifications is well-documented (see, e.g., Morris 1980). With aperture as the independent variable, for a 25-cm telescope, the Morris (1973) formulae deliver a –0.35 magnitude correction for reflectors and a –1.0 magnitude one for refractors. In a study of the brightness of 96P/Machholz, I found that magnification artifact can be reasonably compensated for with a –1.25 log (M/10) correction, where M is magnification normalized to 10, and little or no correction for M < 10 (Marcus 2007a). The issue of whether or not to employ an "aperture" or "magnification" correction for comet light curves has been debated by analysts. The visual m_1 observations plotted in Figure 1 have not been corrected for magnification artifact. However, because C/2010 X1 has been a difficult faint and diffuse object generally requiring substantial magnifications, for forecast purposes, I instead elect to employ a correction of –0.75 magnitude and to represent the adjusted observations as the heavy solid trend line in the upper left of Figure 1. This line is described by the equation $H_1 = 8.0 + 2.5\ n \log r$, where the absolute magnitude is 8 and the slope is n = 4.

Figure 2 presents the baseline total magnitude forecast based on Equation 5, which takes into account the dust-to-gas light ratio, δ_{90}, adopted here as 0.15 (Section 2.2). This forecast, shown as the solid line, is used, along with predicted forward-scattering enhancement (Section 3), to generate the magnitudes in the ephemerides in Section 4. The dotted line shows the dust magnitude, described by $H_{dust}(r) = (H_{dust})_0 + 2.5\ m \log r$, in which the absolute dust magnitude is $(H_{dust})_0 = 10.2$ and the index of dust brightening is m = 3. With the gas contribution, the total absolute magnitude is $H_0 = 8.0$ at log r = 0. Note the prominent "bow" in the predicted baseline total magnitude, in which the current index of brightening, at n = 4, declines to n = 3 beyond log r = 0. Were the comet to venture closer to the sun than its actual perihelion distance, n would decline further to 2 (Figure 2). As the comet recedes from the sun, the n slope steepens. For C/2010 X1, the total magnitude expression in Equation 5 is in fact well approximated by a broken power law, with $H_0 = 8.0$ and n = 4 for $r \geq 1$ AU (the forecast line in Figure 1) and n = 3 for r < 1 AU.

3. Forward-Scattering Brightness Enhancement

As before (Marcus 2007a, c), the brightness enhancement due to forward-scattering of sunlight by the dust is modeled with the modified compound Henyey-Greenstein scattering (or "phase") function

$$\Phi(\theta) = \frac{\delta_{90}}{1+\delta_{90}}\left[k\left(\frac{1+g_f{}^2}{1+g_f{}^2-2g_f\cos\theta}\right)^{3/2} + (1-k)\left(\frac{1+g_b{}^2}{1+g_b{}^2-2g_b\cos\theta}\right)^{3/2} + \frac{1}{\delta_{90}}\right], \quad (7)$$

where θ (= 180° – β) is the scattering angle, $0 \le g_f < 1$ and $-1 < g_b \le 0$ are the forward-scattering and backward-scattering asymmetry factors, $0 \le k < 1$ is the partitioning coefficient between forward and backward scattering and δ_{90} is the dust-to-gas light ratio. The magnitude of the brightness enhancement is

$$m_{\Phi(\theta)} = -2.5\log\Phi(\theta). \quad (8)$$

For simplicity, δ_{90} rather than $\delta_{90}(r)$ (Equation 2) is used here because over the 0.5 AU $\le r \le$ 1.0 AU interval in which significant forward-scattering occurs, $\delta_{90}(r) \approx \delta_{90}$. The extremely low δ_{90} = 0.15 value adopted for C/2010 X1 blunts the anticipated forward-scattering magnitude enhancement. At θ_{min} = 3.1° as viewed from earth, $m_{\Phi(\theta)} = -5.8$ from Equations 7 and 8. In contrast, if the comet were "dusty," with δ_{90} = 10, then $m_{\Phi(\theta)}$ would be –7.9.

4. The SOHO and STEREO Spacecraft

The SOHO ("Solar and Heliospheric Observatory") spacecraft is in solar orbit about 0.01 AU from Earth at the Earth-Sun L_1 Lagrange point. Its two LASCO coronagraphs, C2 and C3, have circular fields of view of 1.5° and 8° radius, respectively, centered on the Sun. The C3 CCD chip and clear filter combination is red-sensitive.

The STEREO-A and STEREO-B ("Solar Terrestrial Relations Observatory") spacecraft are in circular orbits around the Sun in the Earth's orbit plane, the "A" satellite "ahead" of Earth, and the "B" satellite "behind" Earth. At the present time, they each are about 95° from Earth and on opposite sides of the Sun from each other. Their "heliospheric imager" (HI) cameras look at the space between the Sun and the Earth, so that STEREO-A looks eastward and STEREO-B looks westward of the sun. The HI1-A and HI1-B cameras have square fields covering 4° to 24° solar elongation. They typically take 40 summed 40 s exposures for an image, giving a limiting magnitude of roughly 13 (K. Battams, Naval Research Laboratory, personal communication). The HI2-A and HI2-B cameras have circular fields covering 24° to 94° solar elongation (see http://sungrazer.nrl.navy.mil/index.php?p=images/secchi_overview.jpg). The STEREO bandpasses are fairly similar to an R bandpass, although a "blue leak" at ~0.4 μm can transmit emissions from CN and C_3 (M. Knight, personal communication). Comet C/2010 X1 will be visible in the HI1 and HI2 cameras from both STEREO satellites. In addition, each satellite has

a pair of coronagraphs, with fields of view of radii 1° (COR-1) and 4° (COR2) (Howard et al. 2008). The comet enters only the STEREO-A coronagraph fields.

5. Ephemerides for Earth, SOHO, and STEREO-A and STEREO-B with Forward-Scattering Brightness Enhancement

Ephemerides for the comet's position based from Earth were computed using the Minor Planet & Comet Ephemeris Service (online at http://www.minorplanetcenter.org/iau/MPEph/MPEph.html) of the IAU Minor Planet Center in Cambridge, MA. Ephemerides for the comet as viewed from the spacecraft were computed using the Solar System Dynamics "Horizons Web-Interface" program (online at http://ssd.jpl.nasa.gov/horizons.cgi), sponsored by NASA, Jet Propulsion Laboratory, and California Institute of Technology, Pasadena, CA. The "Observer Locations" in the Horizons program for the SOHO, STEREO-A, and STEREO-B spacecraft are coded as"500@-21," "500@-234," and "500@-235" respectively. The forecast total visual magnitude, from Equations 5-8 , is

$$m_1 = H_1(r) + m_{\Phi(\theta)} = H_0 + 5\log\Delta + 2.5m\log r - 2.5\log\left[\frac{1+\delta_{90}(r)^{-1}}{1+\delta_{90}{}^{-1}}\right] + m_{\Phi(\theta)}, \qquad (9)$$

with $H_0 = 8$, $m = 3$, and $\delta_{90} = 0.15$. Here Δ represents comet-earth or comet-spacecraft distance in AU. $\delta_{90}(r)$ is from Equation 2. For the $m_{\Phi(\theta)}$ term, the values for the parameters of the scattering function, $\Phi(\theta)$, are taken as $g_f = +0.9$, $g_b = -0.6$, $k = 0.95$, and $\delta_{90} = 0.15$ for the visual passband, and 0.5 for the satellite clear/unfiltered or red (R) filter images. The lower δ_{90} value for the visual passband reflects the stronger influence of the C_2 Swan emission relative to the broader more red-sensitive CCD passbands for the satellites. The greater dust-to-gas light ratios for the satellite cameras means that the dust scattering function is less blunted by C_2 and other gas emission, so that for them, forward-scattering brightness enhancement will be somewhat more accentuated. The generally reddish color of comet dust will also produce slightly brighter magnitudes for C/2010 X1 in the satellite images than in the V system. After Sostero (Marcus 2007c), this difference normally amounts to V = R + 0.4 magnitude, but because C/2010 X1 is so gassy (with C_2 emission brightening the V band relatively more), this difference may be less.

Tables 1-4 give ephemerides for C/2010 X1 as viewed from Earth, SOHO, STEREO-A, and STEREO-B. They are not meant to be comprehensive, but rather to provide only an overview of the projected baseline brightness and forward-scattering brightness magnitude enhancements (and total magnitude) at appropriately spaced intervals. Ephemerides for locating the comet at more closely-spaced intervals are accessible and easily generated at the above websites for readers who wish to do so. In Tables 1, 3 and 4, The columns list the date in Universal Time (UT), right ascension, declination, earth distance, sun distance, elongation, scattering angle (= 180° – phase angle), magnitude enhancement due to forward-scattering, and the predicted total magnitude (baseline + forward-scattering enhancement). Table 2 gives the comet's offset from the Sun in elongation and position angle, ρ, measured counterclockwise from north, magnitude due to forward-scattering enhancement, and total magnitude for SOHO

and Earth. Note that these entries are virtually identical because the SOHO satellite is so close to the Earth (see above).

5.1 View From Earth (Tables 1, 2)

Over summer, the comet's elongation steadily decreases as it sinks into evening twilight, falling below 40° elongation by Aug. 8 at $m_1 = 9.5$ (Table 1). The comet will reach minimum scattering angle on Sep. 26.8 UT at $\theta_{min} = 3.1°$ and $\varepsilon = 1.9°$, when it reaches its maximum forward-scattering surge in brightness of –5.8 magnitudes (or 210-fold) from a baseline of 4.3 (giving $m_1 = -1.5$). Table 2 provides a high resolution ephemeris with the comet's offset from the sun (elongation, position angle) in this extreme forward-scattering geometry, but it is unlikely that daylight sightings will be possible (see Section 6). If attempts are made, extreme caution should be exercised, with the Sun securely shielded by a building or equivalent obstructing agent, because of the obvious danger of accidental eye damage. C/2010 X1 emerges from morning twilight in early October, when it may be visible to the naked eye in the morning sky with slight (~ –0.5 to –1.0) forward-scattering brightness enhancement. It remains in forward-scattering geometry ($\theta \leq 90°$) through mid-October. Approaching earth, it passes closest on Oct. 16.83 UT at $\Delta_{min} = 0.234$ AU (and $\theta = 86.3°$, $\varepsilon = 72.7°$, and $m_1 = 5.7$) on its way to opposition on Nov. 22.95 UT at $\varepsilon = 175.1°$, $\theta = 177.0°$, $\Delta = 0.597$ AU, r = 1.583 AU and $m_1 = 8.7$ (this includes an expected –0.5 magnitude enhancement due to backscattering). The comet follows the ecliptic westward into the evening sky, sinking below $\varepsilon = 40°$ on 2012 Apr. 18 at $m_1 = 18.5$.

5.2 View from SOHO (Table 2)

The comet enters the SOHO LASCO C3 coronagraph field (when $\varepsilon < 8°$) Sep. 23.6, reaching a minimum elongation $\varepsilon_{min} = 1.9°$ and minimum scattering angle $\theta_{min} = 3.1°$ on Sep. 26.8 UT. In this extreme forward-scattering geometry, the magnitude brightness enhancement should be –6.8 magnitudes (or 520-fold!) from baseline. Within the C3 field itself, the surge will amount to –2.7 magnitudes (cf. Table 2). The comet does not approach the sun sufficiently closely ($\varepsilon_{min} > 1.5°$) to be visible in the C2 coronagraph field. The comet exits the C3 field on Sep. 29.7 UT.

5.3 View from STEREO-A (Table 3)

Moving eastward as it passes behind the Sun, C/2010 X1 will first become visible to STEREO-A in the coronagraphs, entering the COR2 and COR1 fields on Aug. 20.5 UT and 26.5 UT, respectively, and exiting the COR1 and COR2 fields on Aug. 28.7 UT and Sep. 2.0, respectively. Unlike for Earth, SOHO, and STEREO-B, the comet does not enter forward-scattering geometry as viewed from STEREO-A. However, STEREO-A will see a backscattering brightness enhancement of –0.6 magnitude when it reaches superior conjunction with the Sun at $\theta_{max} = 178.9°$ and $\varepsilon_{min} = 0.7°$ on Aug. 27.55 UT. With coronograph limiting magnitudes of ~7-8 (K. Battams and M. Knight, personal communications), the comet may well not be visible in their fields. As C/2010 X1 exits COR2, it enters and traverses the HI1-A camera field, exiting it and entering the HI2-A camera field on Sep. 22 UT. Relative to the Sun,

it continues an increasingly slow eastward jaunt, reaching a maximum elongation of 49.1° on Nov. 7.40 UT before heading slowly back toward the Sun.

5.4 View from STEREO-B (Table 4)

The apparition of C/2010 X1 is dramatic at STEREO-B, featuring a very close approach to the spacecraft in increasing forward-scattering geometry. The comet approaches the spacecraft from behind, passing east and south of it, with a minimum approach distance of Δ_{min} = 0.049 AU on Jul. 31.53 at θ = 89.2° and r = 1.043 AU. Heading between the craft and the Sun, the comet reaches minimum scattering angle θ_{min} = 7.3° on Aug. 13.63 UT, and minimum elongation ε_{min} = 5.7° at about the same time, too large for the comet to enter the coronagraph fields. Despite the fact that the comet is east of the sun in this period, images could be obtained if the spacecraft "rolls" to an appropriate angle (Battams, personal communication). Otherwise, in the normal default spacecraft configuration, the comet enters the HI1-B field on Aug. 15 UT, when θ = 8.5°, and forward-scattering brightness enhancement is $m_{\Phi(\theta)} = -5.4$ (or 140–fold) and $m_1 = -1.1$ and passes into the HI2-B field on Sep. 3 UT (at θ = 54.5°, $m_{\Phi(\theta)} = -0.7$, $m_1 = 4.4$), where it remains as it attains increasing westward elongation through the end of the year.

6. The Unlikelihood of the Visibility of C/2010 X1 in Daylight

Venturing as it does into such extreme forward-scattering geometry, will C/2010 X1 become visible in daylight as did C/2006 P1 (McNaught) (Marcus 2007b, c)? In a companion paper (Marcus, 2011), I presented a model to predict the limiting magnitude of a comet in daylight:

$$m_{lim}(\varepsilon, M, \Delta, r) = (m_{lim})_0 + 2.5(\log\varepsilon + \log M + \log\Delta - 1.5\log r - 0.43). \qquad (10)$$

The threshold visibility depends upon the diameter of the dust coma, modeled as $D = 8' \times r^{1.5}$ (as viewed at Δ = 1 AU); the background sky brightness, a function of the solar elongation, ε (in degrees); and the global magnification of the coma, $\mu = M\Delta^{-1}$, where M is instrument magnification (M = 1 for naked eye), and Δ is earth distance in AU. $(m_{lim})_0$ is the naked eye limiting magnitude for a coma of 3′ or smaller size, taken as –5.6 at ε = 1°. The model incorporates Piper's psychophysical law, in which the visual nervous system suffers incomplete spatial summation for stimuli larger than 3′ at daylight sky backgrounds (Marcus 2011). While in forward-scattering geometry, the coma of C/2010 X1 should exceed 3′ for the naked eye.

Figure 3 plots the daylight limiting magnitude from Equation 10 for C/2010 X1 at its maximum brightness near the sun at θ_{min} for M = 1 and M = 10. Also plotted is the comet's magnitude as predicted by Equation 5. Each peak at the time that the comet reaches minimum scattering angle and elongation, which occurs 16 days beyond perihelion. Each peak is due to forward-scattering – in the case of the comet's magnitude, by coma dust grains, and in the case of the limiting magnitude, by atmospheric aerosols and particulates which contribute increasingly to sky brightness at decreasing elongation (which is a proxy for the aerosol scattering angle). It is evident from Figure 3 that the comet is not likely to become bright enough to cross the threshold of daylight visibility. The remote possibility that it could become

visible in daylight could only be due an unlikely confluence of favorable factors which include low solar elevation, extremely clear air, and unusually high observer contrast sensitivity.

7. Discussion

Comet C/2010 X1 (Elenin) can be expected to undergo a huge brightness surge due to forward-scattering enhancement as viewed from Earth and the SOHO and STEREO-B spacecraft. However, owing to its intrinsic dimness, as measured by its faint absolute magnitude of $H_0 = 8.0$, this surge will be hardly noticeable as observed from Earth, because when it occurs, the comet will be at low elongations and obscured by twilight, and when close to the sun at small scattering angles, it is intrinsically too faint to become visible in daylight. At most, the observable surge will be −0.5 to −1.0 in early October (Table 1). The best views should be in the STEREO-B satellite fields in August and the SOHO LASCO C3 coronagraph field in late September. Due to forward-scattering by the dust, the magnitude of the coma may reach $m_1 = -1.6$ from STEREO-B, and $m_1 = -2.5$ from SOHO, and any dust tail and antitail should become prominent, accentuated even further by their near co-planarities with Earth's orbit, which should project the tail as a thin but concentrated beam independent of any forward-scattering brightness enhancement.

The magnitude predictions in this paper were generated by two new models. The first is the modified compound Henyey-Greenstein function for forward-scattering brightness enhancement of comets as presented in Papers I and II (Marcus 2007a, 2007c). The second, presented here, characterizes the *baseline* light curve of a comet as a function of the dust-to-gas light ratio, $\delta_{90}(r)$, which varies with r, on the assumption that the dust magnitude varies linearly with log r. This baseline model produces a "bowed" *total* magnitude (dust + gas) light curve which is particularly prominent for comets such as C/2010 X1 which have low δ_{90} values, as illustrated in Figure 2. All predictions, of course, must be accompanied by a word of caution. The baseline brightness forecast has some uncertainty owing to uncertainties in the parameters H_0 and δ_{90} in the model of Equation 9, and the projection through a large range of log r. This baseline could be brighter or dimmer than predicted in Equation 5 (as shown by the offsets in Figure 3), and the comet could always disintegrate altogether (!), although its intrinsic size ($H_0 = 8$) suggests that it will survive perihelion passage (Bortle 1991).

The extreme "gassiness" of C/2010 X1, reflected in its unusually small δ_{90} parameter, will blunt the forward-scattering brightness surge, which nevertheless should still be considerable because the comet reaches such very small scattering angles as viewed from Earth, SOHO, and STEREO-B [see $m_{\Phi(\theta)}$ in Tables 1, 2, and 4]. Morphologically such gassy comets often appear as "lollipops," with thin, inconspicuous plasma tails representing the "sticks." The extreme forward-scattering geometry should nevertheless bring out the dust features in C/2010 X1. The prospect of being able to view and image the comet simultaneously from the different spacecraft and from Earth offers an unprecedented opportunity to characterize the scattering function of a cometary coma at small scattering angles.

7. Acknowledgments

I thank Jon Giorgini, Jet Propulsion Laboratory, Pasadena, California, for extending the coordinates of the SOHO spacecraft in the JPL Horizons ephemeris program; Karl Battams, Naval Research Laboratory, Washington, DC, for discussion of the STEREO cameras and their fields; Matthew Knight, Lowell Observatory, for discussions on filters and capabilities of the satellite cameras; David Schleicher, Lowell Observatory, for communication (via Knight) of preliminary continuum photometry data on C/2010 X1; Knight and Battams for reviews of the manuscript; and the Editor for supplying provisional magnitude estimates of C/2010 X1 and for his editorial work on the manuscript.

References

A'Hearn MF, Millis RL, Schleicher DG, Osip DJ, Birch PV (1995). The ensemble properties of comets: Results from narrowband photometry of 85 comets, 1976-1992. *Icarus* 118:223-270

Bortle JE (1991). Post-perihelion survival of comets with small q. *Int Comet Qrtly* 13:89-91

Ferrín I (2005). Variable-aperture-correction method in cometary photometry. *Intnl Comet Qrtly* 249-255

Howard TA, Nandy D, Koepke AC (2008). Kinematic properties of solar coronal mass ejections: Correction for projection effects in spacecraft coronograph measurements. *J Geophys Res* 113:A01104

Knight MM, A'Hearn MF, Biesecker DA, Faury G, Hamilton DP, Lamy P, Llebaria A (2010). Photometric study of the Kreutz comets observed by *SOHO* from 1996 to 2005. *Astron J* 139:929-949

Marcus JN (2007a). Forward-scattering enhancement of comet brightness. I. Background and model. *Intnl Comet Quart* 29:39-66

Marcus JN (2007b). C/2006 P1 (McNaught). *IAU Circular* 8793, 2007 Jan. 11

Marcus JN (2007c) Forward-scattering enhancement of comet brightness. II. The light curve of C/2006 P1 (McNaught). *Intnl Comet Quart* 29:119-130

Marcus JN (2011). The daylight visibility of comets. *Intnl Comet Qrtly*, submitted

Morris CS (1973). On aperture corrections for comet magnitude estimates. *Publ Astron Soc Pacif* 85:470-473

Morris CS (1980). The apparition of comet Bradfield (1979*l*). *Intnl Comet Qrtly* 2:23-26

Newburn RL Jr (1981). A new calibration of the semi-empirical photometric theory for Halley and other comets. *Adv Space Res* 4, 185

Sostero G, Milani G (2011). Strange behavior of C.2010 X1 (Elenin). Message 17396, Comets-m1 (http://tech.groups.yahoo.com/group/comets-ml/message/17396)

Williams GV (2011). Observations and orbits of comets. *Minor Planet Electronic Circular* 2011-N34, 2011 July 7

Table 1. Ephemerides for C/2010 X1 (Elenin), as Viewed from Earth, with Forward-Scattering Brightness Enhancement

2011 (UT)	$\alpha_{J2000.0}$ (h m s)	$\delta_{J2000.0}$ (° ′ ″)	Δ (AU)	r (AU)	ε (°)	θ (°)	$m_{\Phi(\theta)}$	m_1
Jul. 18.0	11 03 22.5	+04 43 41	1.659	1.276	50.3	142.3	+0.0	10.1
Jul. 23.0	11 10 44.0	+03 58 18	1.613	1.191	47.5	141.1	+0.0	9.8
Jul. 28.0	11 18 48.7	+03 07 58	1.560	1.105	44.9	139.6	+0.0	9.4
Aug. 02.0	11 27 38.6	+02 12 30	1.500	1.017	42.5	137.6	+0.0	9.0
Aug. 07.0	11 37 15.2	+01 11 53	1.433	0.930	40.3	135.1	+0.1	8.6
Aug. 12.0	11 47 38.9	+00 06 14	1.356	0.843	38.3	131.8	+0.1	8.1
Aug. 17.0	11 58 48.4	−01 03 54	1.271	0.757	36.6	127.2	+0.1	7.6
Aug. 22.0	12 10 36.3	−02 17 08	1.176	0.675	34.9	120.9	+0.1	7.1
Aug. 27.0	12 22 43.2	−03 30 17	1.071	0.600	33.4	112.2	+0.0	6.5
Sep. 01.0	12 34 22.7	−04 37 01	0.955	0.538	31.7	100.2	+0.0	6.0
Sep. 06.0	12 44 05.5	−05 25 54	0.831	0.496	29.3	84.5	−0.0	5.4
Sep. 11.0	12 49 33.8	−05 40 11	0.706	0.483	25.8	65.4	−0.2	4.9
Sep. 16.0	12 48 16.1	−05 01 26	0.587	0.500	20.4	44.6	−0.5	4.1
Sep. 21.0	12 38 24.3	−03 14 52	0.482	0.544	12.6	23.7	−1.9	2.6
Sep. 26.0	12 19 04.9	−00 10 27	0.396	0.608	2.7	4.4	−5.5	−1.1
Oct. 01.0	11 49 37.5	+04 18 28	0.328	0.683	11.8	17.4	−2.7	1.6
Oct. 03.0	11 34 46.8	+06 30 00	0.306	0.716	18.0	25.5	−1.7	2.6
Oct. 05.0	11 18 05.5	+08 54 17	0.287	0.749	24.7	33.9	−1.0	3.3
Oct. 07.0	10 59 22.5	+11 29 34	0.270	0.783	31.9	42.4	−0.6	3.7
Oct. 09.0	10 38 40.6	+14 12 58	0.257	0.816	39.6	51.1	−0.4	4.0
Oct. 11.0	10 15 57.5	+17 00 13	0.247	0.852	47.7	60.0	−0.2	4.2
Oct. 13.0	09 51 19.0	+19 45 45	0.239	0.887	56.1	69.0	−0.1	4.3
Oct. 15.0	09 24 58.5	+22 23 05	0.235	0.922	64.7	78.1	−0.1	4.5
Oct. 17.0	08 57 19.1	+24 45 35	0.234	0.957	73.5	88.0	−0.0	4.7
Oct. 19.0	08 28 53.2	+26 47 31	0.236	0.992	82.2	95.8	+0.0	4.9
Oct. 21.0	08 00 19.4	+28 25 04	0.240	1.027	90.7	104.2	+0.0	5.0
Oct. 23.0	07 32 18.2	+29 36 50	0.248	1.062	98.9	112.2	+0.0	5.2
Oct. 25.0	07 05 25.9	+30 23 43	0.257	1.097	106.7	119.7	+0.1	5.5
Oct. 27.0	06 40 10.7	+30 48 27	0.270	1.131	114.1	126.7	+0.1	5.7
Oct. 29.0	06 16 50.8	+30 54 45	0.284	1.166	121.1	133.1	+0.1	5.9
Oct. 31.0	05 55 34.6	+30 46 35	0.301	1.200	127.6	139.1	+0.1	6.2
Nov. 05.0	05 11 16.0	+29 46 16	0.350	1.286	142.1	151.8	+0.0	6.7
Nov. 10.0	04 37 58.2	+28 20 56	0.408	1.370	154.4	161.8	−0.0	7.3
Nov. 15.0	04 13 09.1	+26 53 23	0.475	1.453	164.8	169.7	−0.1	7.9
Nov. 20.0	03 54 38.2	+25 33 21	0.549	1.535	173.0	175.5	−0.1	8.4
Nov. 25.0	03 40 49.7	+24 24 10	0.630	1.616	174.1	176.4	−0.1	8.9
Nov. 30.0	03 30 36.3	+23 26 20	0.718	1.695	168.0	173.1	−0.1	9.4
Dec. 05.0	03 23 09.7	+11 39 10	0.811	1.774	161.5	169.8	−0.1	9.9
Dec. 10.0	03 17 54.2	+22 01 30	0.910	1.851	155.2	167.1	−0.0	10.4
Dec. 15.0	03 14 23.0	+21 32 07	1.014	1.927	149.3	164.9	−0.0	10.8
Dec. 20.0	03 12 16.0	+21 09 50	1.123	2.003	143.7	163.1	−0.0	11.2
Dec. 25.0	03 11 18.7	+20 53 38	1.237	2.077	138.4	161.7	−0.0	11.6
Dec. 30.0	03 11 19.7	+20 42 38	1.354	2.150	133.2	160.5	−0.0	12.0

Table 2. Offset Ephemerides for C/2010 X1 (Elenin), as Viewed from Earth in Daylight and from the SOHO Spacecraft, with Forward-Scattering Brightness Enhancement

2011 (UT)	EARTH (Visual)					SOHO (Clear Filter, V-Equivalent)				
	ε (°)	ρ (°)	θ (°)	$m_{\Phi(\theta)}$	m_1	ε (°)	ρ (°)	θ (°)	$m_{\Phi(\theta)}$	m_1
Sep. 23.5	7.8	104.2	13.7	−3.3	1.1	08.2	104.7	14.2	−4.2	0.2
Sep. 24.0	6.7	102.0	11.7	−3.7	0.7	07.1	102.6	12.3	−4.6	−0.2
Sep. 24.5	5.7	98.8	9.7	−4.1	0.3	06.1	99.8	10.3	−5.0	−0.7
Sep. 25.0	4.6	94.1	7.8	−4.6	−0.2	05.0	95.5	8.4	−5.5	−1.1
Sep. 25.5	3.6	86.6	6.0	−5.1	−0.7	03.9	88.9	6.5	−6.0	−1.6
Sep. 26.0	2.7	73.0	4.4	−5.5	−1.1	02.9	77.2	4.8	−6.4	−2.1
Sep. 26.5	2.0	47.7	3.3	−5.8	−1.4	02.2	55.0	3.5	−6.7	−2.4
Sep. 27.0	2.0	11.6	3.2	−5.8	−1.5	02.0	19.6	3.1	−6.8	−2.5
Sep. 27.5	2.7	344.8	4.2	−5.6	−1.2	02.5	348.8	4.0	−6.6	−2.3
Sep. 28.0	3.7	329.6	5.8	−5.1	−0.8	03.5	331.8	5.5	−6.2	−2.0
Sep. 28.5	4.9	321.4	7.6	−4.7	−0.3	04.7	322.2	7.3	−5.8	−1.5
Sep. 29.0	6.2	316.5	9.5	−4.2	0.1	06.0	317.1	9.2	−5.3	−1.0
Sep. 29.5	7.5	313.2	11.4	−3.8	0.6	07.4	313.5	11.2	−4.8	−0.5
Sep. 30.0	8.9	310.8	13.4	−3.4	1.0	08.8	311.0	13.2	−4.4	−0.1

Table 3. Ephemerides for C/2010 X1 (Elenin), as Viewed from STEREO-A, with Forward-Scattering Brightness Enhancement

2011-12 (UT)	$\alpha_{J2000.0}$ (h m s)	$\delta_{J2000.0}$ (° ′ ″)	Δ (AU)	r (AU)	ε (°)	θ (°)	$m_{\Phi(\theta)}$	m_1
Aug. 20.0	16 07 20.8	−21 40 05	1.666	0.707	4.2	174.3	−0.2	7.8
Aug. 22.0	16 20 06.3	−22 10 16	1.636	0.675	3.3	175.3	−0.2	7.6
Aug. 24.0	16 33 26.6	−22 37 34	1.607	0.644	2.3	176.6	−0.2	7.4
Aug. 26.0	16 47 21.9	−23 01 24	1.579	0.615	1.2	178.1	−0.2	7.2
Aug. 28.0	17 01 52.5	−23 21 10	1.552	0.587	0.7	178.8	−0.2	7.0
Aug. 30.0	17 16 57.4	−23 36 12	1.525	0.561	1.8	176.9	−0.2	6.9
Sep. 01.0	17 32 35.4	−23 45 50	1.499	0.538	3.2	174.2	−0.2	6.7
Sep. 03.0	17 48 43.9	−23 49 26	1.474	0.519	4.8	171.0	−0.1	6.6
Sep. 06.0	18 13 45.9	−23 42 14	1.438	0.496	7.4	163.4	−0.1	6.5
Sep. 11.0	18 56 58.7	−22 54 14	1.381	0.483	12.2	154.9	+0.0	6.5
Sep. 16.0	19 40 42.6	−21 16 40	1.332	0.500	17.3	144.9	+0.1	6.6
Sep. 21.0	20 23 33.9	−18 57 04	1.293	0.544	22.4	137.3	+0.1	6.8
Sep. 26.0	21 04 36.6	−16 03 32	1.271	0.608	27.5	132.8	+0.1	7.0
Oct. 01.0	21 43 16.8	−12 47 25	1.267	0.684	32.2	131.1	+0.1	7.4
Oct. 06.0	22 19 16.5	−09 20 39	1.283	0.766	36.5	131.3	+0.1	7.8
Oct. 11.0	22 52 27.1	−05 54 03	1.317	0.852	40.3	132.8	+0.1	8.2
Oct. 16.0	23 22 49.0	−02 36 05	1.367	0.939	43.4	135.0	+0.1	8.6
Oct. 21.0	23 50 29.9	+00 27 49	1.432	1.027	45.8	137.5	+0.1	9.0
Oct. 26.0	00 15 42.5	+03 14 55	1.509	1.114	47.5	140.2	+0.1	9.4
Oct. 31.0	00 38 42.0	+05 44 37	1.596	1.200	48.6	142.8	+0.1	9.8
Nov. 05.0	00 59 44.0	+07 57 36	1.691	1.286	49.1	145.4	+0.1	10.2
Nov. 10.0	01 19 03.7	+09 55 15	1.792	1.370	49.1	147.8	+0.1	10.6
Nov. 15.0	01 36 54.9	+11 39 13	1.898	1.453	48.6	150.0	+0.1	10.9
Nov. 20.0	01 53 29.6	+13 11 09	2.007	1.535	47.8	152.2	+0.1	11.2
Nov. 25.0	02 08 58.4	+14 32 36	2.119	1.615	46.6	154.2	+0.0	11.5
Nov. 30.0	02 23 30.3	+15 44 56	2.232	1.695	45.1	156.2	+0.0	11.8
Dec. 05.0	02 37 12.8	+16 49 20	2.346	1.773	43.4	158.0	+0.0	12.1
Dec. 10.0	02 50 12.4	+17 46 47	2.460	1.851	41.5	159.8	+0.0	12.4
Dec. 15.0	03 02 34.3	+18 38 09	2.574	1.927	39.3	161.5	−0.0	12.6
Dec. 20.0	03 14 23.1	+19 24 09	2.686	2.003	37.0	163.1	−0.1	12.9
Dec. 25.0	03 25 42.4	+20 05 22	2.797	2.077	34.6	164.7	−0.1	13.1
Dec. 30.0	03 36 35.4	+20 42 18	2.906	2.151	32.0	166.3	−0.1	13.3

Table 4. Ephemerides for C/2010 X1 (Elenin), as Viewed from STEREO-B, with Forward-Scattering Brightness Enhancement

2011-12 (UT)	$\alpha_{J2000.0}$ (h m s)	$\delta_{J2000.0}$ (° ′ ″)	Δ (AU)	r (AU)	ε (°)	θ (°)	$m_{\Phi(\theta)}$	m_1
Jul. 31.5	07 57 43.9	−12 51 17	0.049	1.043	89.9	92.7	+0.0	1.6
Aug. 01.0	07 18 12.8	−10 08 56	0.050	1.035	79.5	82.2	−0.1	1.5
Aug. 01.5	06 41 29.3	−07 19 24	0.052	1.026	69.6	72.3	−0.2	1.5
Aug. 02.0	06 08 53.1	−04 37 23	0.056	1.017	60.7	63.4	−0.4	1.4
Aug. 02.5	05 40 49.4	−02 12 20	0.060	1.009	52.9	55.6	−0.6	1.3
Aug. 03.0	05 17 04.9	−00 07 35	0.066	1.000	46.2	48.9	−0.9	1.2
Aug. 03.5	04 57 07.8	+01 37 24	0.072	0.991	40.5	43.2	−1.1	1.1
Aug. 04.0	04 40 21.8	+03 04 58	0.078	0.982	35.7	38.4	−1.4	1.0
Aug. 05.0	04 14 11.6	+05 19 02	0.093	0.965	28.1	30.7	−2.0	0.7
Aug. 06.0	03 55 02.2	+06 54 08	0.108	0.947	22.3	24.8	−2.6	0.4
Aug. 07.0	03 40 34.8	+08 03 44	0.124	0.930	17.9	20.2	−3.2	0.0
Aug. 09.0	03 20 26.1	+09 37 14	0.157	0.895	11.5	13.5	−4.3	−0.7
Aug. 11.0	03 07 11.7	+10 36 39	0.197	0.860	7.4	9.1	−5.8	−1.4
Aug. 13.0	02 57 55.2	+11 17 54	0.227	0.825	5.8	7.3	−5.8	−1.6
Aug. 15.0	02 51 08.4	+11 48 43	0.264	0.791	6.4	8.5	−5.4	−1.1
Aug. 17.0	02 46 03.8	+12 13 14	0.301	0.757	8.2	11.5	−4.7	−0.3
Aug. 22.0	02 38 18.0	+13 01 06	0.400	0.675	13.6	21.6	−3.0	1.7
Aug. 27.0	02 35 32.6	+13 43 55	0.507	0.600	18.3	43.7	−1.1	3.8
Sep. 01.0	02 37 05.6	+14 31 48	0.625	0.538	22.1	48.1	−0.9	4.1
Sep. 06.0	02 43 02.6	+15 30 15	0.755	0.496	24.9	64.6	−0.4	4.8
Sep. 11.0	02 53 22.1	+16 40 03	0.892	0.483	26.6	82.3	−0.1	5.4
Sep. 16.0	03 07 16.3	+17 56 27	1.030	0.500	27.4	99.1	+0.1	6.0
Sep. 21.0	03 23 17.2	+19 11 51	1.163	0.544	27.8	113.0	+0.1	6.5
Sep. 26.0	03 39 58.9	+20 20 16	1.286	0.608	28.1	123.6	+0.1	7.1
Oct. 01.0	03 56 24.6	+21 19 00	1.400	0.684	28.4	131.3	+0.1	7.6
Oct. 06.0	04 12 05.5	+22 07 49	1.504	0.766	29.0	136.8	+0.1	8.1
Oct. 11.0	04 26 50.1	+22 47 33	1.598	0.852	29.9	140.8	+0.1	8.6
Oct. 16.0	04 40 35.8	+23 19 26	1.685	0.939	30.9	143.6	+0.1	9.0
Oct. 21.0	04 53 23.8	+23 44 42	1.765	1.027	32.3	145.7	+0.1	9.4
Oct. 26.0	05 05 17.3	+24 04 27	1.838	1.114	33.8	147.2	+0.1	9.8
Oct. 31.0	05 16 19.4	+24 29 39	1.905	1.200	35.5	148.3	+0.1	10.2
Nov. 05.0	05 26 34.0	+24 31 06	1.965	1.286	37.5	149.1	+0.1	10.5
Nov. 10.0	05 36 03.6	+24 39 28	2.020	1.370	39.6	149.7	+0.1	10.8
Nov. 15.0	05 44 51.1	+24 45 21	2.069	1.453	41.9	150.1	+0.1	11.1
Nov. 20.0	05 52 58.6	+24 49 12	2.113	1.535	44.2	150.4	+0.1	11.4
Nov. 25.0	06 00 28.0	+24 51 28	2.151	1.615	46.8	150.7	+0.1	11.6
Nov. 30.0	06 07 20.6	+24 52 30	2.185	1.695	49.5	150.9	+0.1	11.8
Dec. 05.0	06 13 37.5	+24 52 37	2.213	1.774	52.4	151.1	+0.1	12.1
Dec. 10.0	06 19 19.4	+24 52 06	2.237	1.851	55.4	151.3	+0.1	12.3
Dec. 15.0	06 24 26.7	+24 51 11	2.257	1.927	58.5	151.5	+0.1	12.4
Dec. 20.0	06 28 59.5	+24 50 06	2.272	2.003	61.8	151.7	+0.1	12.6
Dec. 25.0	06 32 57.7	+24 49 02	2.283	2.077	65.3	151.9	+0.1	12.8
Dec. 30.0	06 36 20.8	+24 48 10	2.291	2.151	68.8	152.3	+0.1	12.9

FIGURE CAPTIONS

Figure 1. Heliocentric magnitude observations of comet C/2010 X1 plotted against the logarithm of the heliocentric distance for CCD and visual various observers. The line is a short-term fit inferred for low magnification binoculars and naked eye. See text for details.

Figure 2. The baseline total magnitude forecast (solid line) for C/2010 X1 (Elenin), without forward-scattering brightness enhancement, as seen in low-power binoculars or by naked eye. The dust component (dashed line) has an assumed slope of m = 3 in Equation 5. The comet's extremely low dust-to-gas light ratio of $\delta_{90} = 0.15$ produces a strong "bow" near r = 1 AU (log r = 0), so that the early slope of brightening of the total magnitude (n = 4) at r > 1 AU should decline as the comet approaches its perihelion at r < 1 AU, and steepen afterwards as it recedes from the sun.

Figure 3. The forecast magnitude of Comet C/2010 X1 (Elenin) as viewed from Earth in extreme forward-scattering geometry from Equation 9 (heavy solid line), with offsets for 1 and 2 magnitudes brighter and dimmer (thin solid lines). The baseline magnitude without forward-scattering enhancement is the heavy shaded line. Also shown is the limiting magnitude for daylight visibility at magnifications of 1 (naked eye) (heavy dashed line) and 10 (light dashed line), after the model in Equation 10. It is unlikely that C/2010 X1 will become visible in daylight.

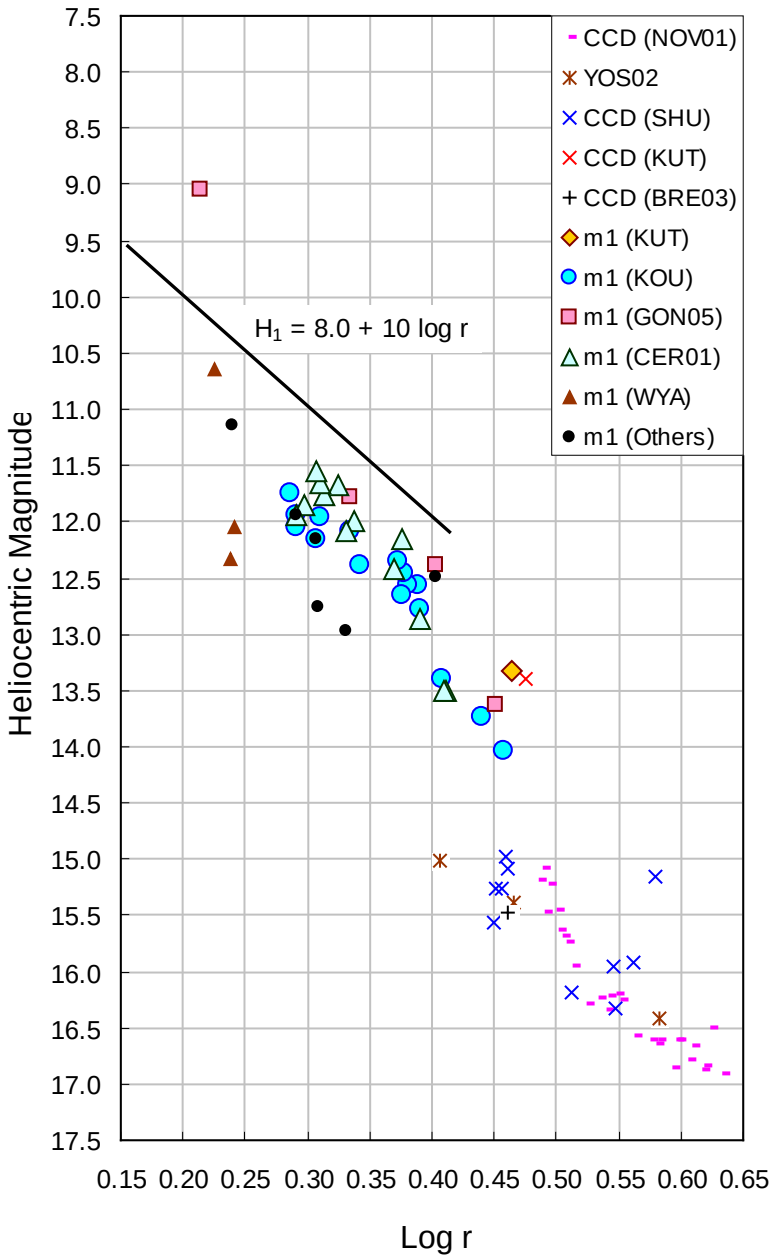
Heliocentric Magnitude
Log r
H_1 = 8.0 + 10 log r
CCD (NOV01)
YOS02
CCD (SHU)
CCD (KUT)
CCD (BRE03)
m1 (KUT)
m1 (KOU)
m1 (GON05)
m1 (CER01)
m1 (WYA)
m1 (Others)
7.5
8.0
8.5
9.0
9.5
10.0
10.5
11.0
11.5
12.0
12.5
13.0
13.5
14.0
14.5
15.0
15.5
16.0
16.5
17.0
17.5
0.15 0.20 0.25 0.30 0.35 0.40 0.45 0.50 0.55 0.60 0.65

Figure 1

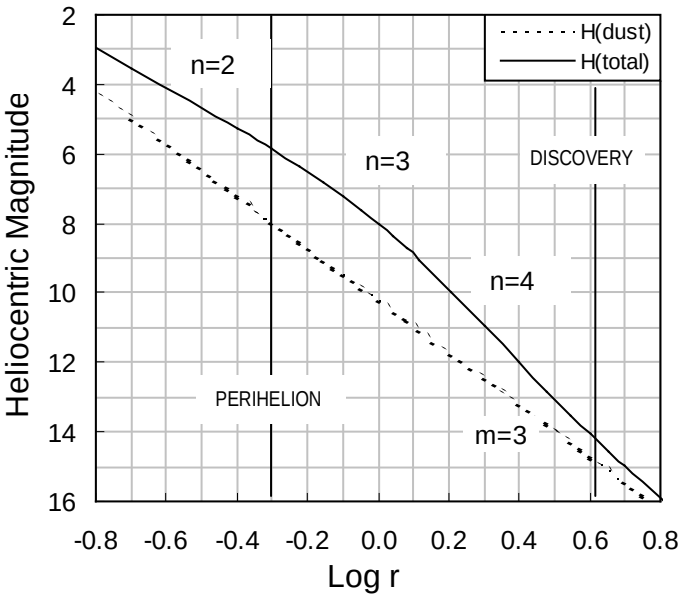
H(dust)
H(total)
n=2
n=3
n=4
m=3
DISCOVERY
PERIHELION
Heliocentric Magnitude
Log r
2
4
6
8
10
12
14
16
-0.8
-0.6
-0.4
-0.2
0.0
0.2
0.4
0.6
0.8

Figure 2

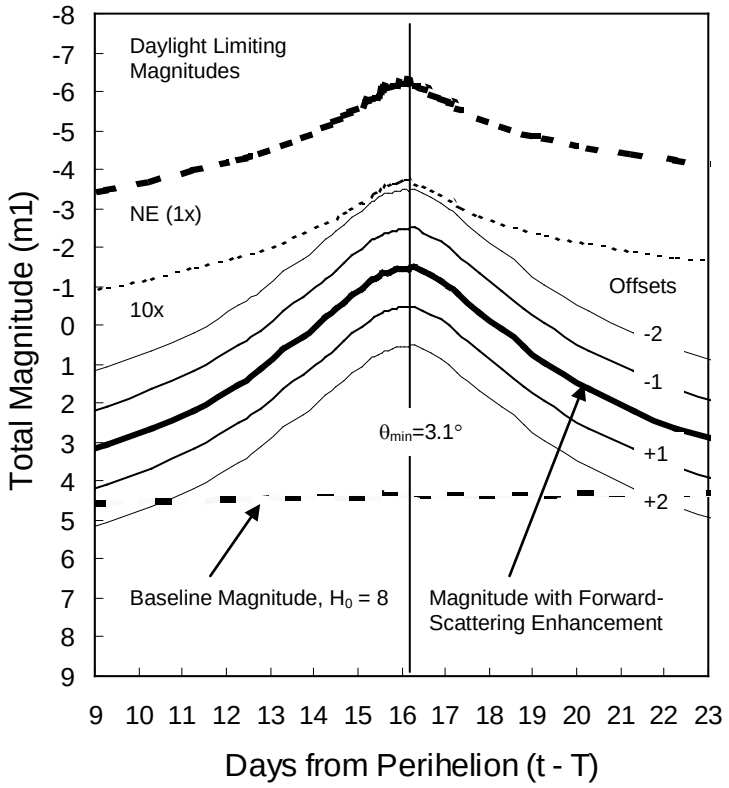
Daylight Limiting Magnitudes
NE (1x)
10x
Offsets
-2
-1
+1
+2
θmin=3.1°
Baseline Magnitude, H0 = 8
Magnitude with Forward-Scattering Enhancement
Total Magnitude (m1)
Days from Perihelion (t - T)
-8
-7
-6
-5
-4
-3
-2
-1
0
1
2
3
4
5
6
7
8
9
9 10 11 12 13 14 15 16 17 18 19 20 21 22 23

Figure 3